HHS Public Access

Author manuscript

Nat Neurosci. Author manuscript; available in PMC 2012 April 01.

Published in final edited form as:

Nat Neurosci. ; 14(10): 1309–1316. doi:10.1038/nn.2927.

Cone photoreceptor contributions to noise and correlations in the retinal output

Petri Ala-Laurila[1,*], **Martin Greschner**[2,*], **E.J. Chichilnisky**[2], and **Fred Rieke**[1]

[1]Howard Hughes Medical Institute and Department of Physiology and Biophysics, University of Washington, Seattle, WA 98195

[2]The Salk Institute, La Jolla, CA 92037

Abstract

Transduction and synaptic noise generated in retinal cone photoreceptors determines the fidelity with which light inputs are encoded, while the readout of cone signals by downstream circuits determines whether this fidelity is used for vision. We examined the impact of cone noise on visual signals by measuring its contribution to correlated noise in primate retinal ganglion cells. Correlated noise was strong in responses of dissimilar cell types with shared cone inputs. The dynamics of cone noise could account for rapid correlations in ganglion cell activity, and the extent of shared cone input could explain correlation strength. Further, correlated noise limited the fidelity with which visual signals were encoded by populations of ganglion cells. Thus a simple picture emerges: cone noise, traversing the retina through diverse pathways, accounts for most of the noise and correlations in the retinal output and constrains how higher centers exploit signals carried by parallel visual pathways.

INTRODUCTION

The sensitivity of cone vision is impressive. For example, the rich palette of colors we perceive relies on discriminating changes in wavelength ~50 times smaller than the width of the cone spectral sensitivity curves [1], and spatial acuity is ~20 times finer than the spacing between cones [2]. Yet some stimuli are too small, too brief, or too weak to resolve. What physiological mechanisms limit visual sensitivity? To answer this question we examined simultaneously two issues that have been investigated largely separately: (1) the noise sources that limit the fidelity of the responses of retinal ganglion cells, which convey visual information to the brain, and (2) the neural mechanisms that underlie the correlated activity of retinal ganglion cells.

First, little is known about the origin and impact of noise in retinal ganglion cells at light levels for which vision is mediated by cones. The importance of noise produced in transduction and transmitter release in cones relative to that of noise introduced by processes

Correspondence: Fred Rieke, rieke@u.washington.edu.

*equal contributions

downstream of the cones has been particularly difficult to resolve. Noise originating from thermal activation of the cone photopigment has been suggested to limit behavioral sensitivity [3,4]; indeed thermal noise is an important factor limiting rod-mediated vision [4–7]. However, the kinetics and magnitude of the noise in the responses of primate cones is inconsistent with an origin in thermal noise [8,9], implying that other mechanisms contribute to cone noise. Synaptic noise originating from statistical variations in vesicle fusion has also been suggested to limit the fidelity of cone-mediated visual signals [10]. Comparison of noise in horizontal cells and ganglion cells in guinea pig retina suggests that both cone noise and post-cone noise contribute substantially to the retinal output [11]. However, cone sensitivity and noise have not been measured under conditions that allow direct comparison with signals in downstream circuits or with behavior. These considerations suggest the value of studying the magnitude, dynamics and propagation of cone noise through the circuitry of the primate retina.

Second, action potentials produced by nearby ganglion cells are often correlated in the absence of modulated light inputs (reviewed in refs. 12–14). Such correlated noise is likely to influence visual signaling by ganglion cells, for example by limiting the effectiveness of averaging inputs from different cells in downstream circuits to reduce noise [15]. Slowly varying correlated noise, particularly prominent in the dark, appears at least partially due to shared inputs to nearby ganglion cells produced by thermal activation of the rod photopigment [16]. More rapid correlated noise, which dominates at cone light levels, must similarly be produced by fluctuations in the responses of retinal neurons, but it is unclear where the fluctuations originate. The rapid dynamics of the correlated noise suggest an origin in a retinal interneuron that provides direct divergent input to nearby ganglion cells [17,18]. Correlated noise in salamander retina persists in the absence of chemical synaptic transmission, indicating that it can be produced in circuits relying exclusively on electrical synapses [19].

We examined the origin of noise in the primate retina at cone light levels, and explored its role in producing correlated noise in the retinal output. The results suggest a simple picture: rapidly varying noise generated by cone photoreceptors produces most of the noise seen in individual ganglion cells, as well as most of the correlated noise between ganglion cells that share cone inputs. This noise in large part determines the fidelity of population visual signals transmitted to the brain.

RESULTS

Correlated noise in the responses of dissimilar cell types

Physiological noise occurs both in cone phototransduction [8,20] and transmitter release [21]. This suggests that correlated noise in the responses of nearby ganglion cells may originate in the cones themselves. To test this hypothesis, we recorded excitatory synaptic inputs from pairs of cells that share little known circuitry other than cones. These experiments were in the presence of steady light producing ~4000 photoisomerizations/cone/sec (R*/cone/sec), a light level 40–100 fold higher than that required to suppress rod input to cones and to ganglion cells [8,22]. All recordings were from ganglion cells in peripheral retina (eccentricity

> 20 deg), meaning that parasol and midget ganglion cells received input, via bipolar cells, from 130–200 cones and 10–30 cones respectively [23].

We started by comparing simultaneously recorded responses of ON and OFF parasol ganglion cells. These cells share no direct excitatory input because signals at the cone output synapse diverge immediately to ON and OFF diffuse cone bipolar cells, which provide excitatory input to ON and OFF ganglion cells respectively [24] (Figure 1a, red and blue circuits in left panel). Figure 1a shows recordings of excitatory synaptic inputs (holding potentials ~−70 mV, see Methods) in response to a randomly-modulated light input followed by a period of constant light. We quantified correlated noise during constant light by computing the crosscorrelation function (Figure 1b; see Methods) - i.e. the (normalized) correlation coefficient between the two signals as a function of the time shift of one signal relative to the other.

The negative peak in the crosscorrelation function in Figure 1b indicates the presence of shared noise, of opposite sign, in the excitatory synaptic inputs to ON and OFF parasol ganglion cells. Such negative correlations are consistent with fluctuations in transmitter release from cones and the opposite polarity of responses of ON and OFF bipolar cells to released transmitter. Fluctuations in the excitatory synaptic input to ON parasol cells led the opposite polarity fluctuations in the input to OFF parasol cells by ~5 ms (crosscorrelation peak time of 5 ± 1 ms, mean ± SEM, n=9) and the two were correlated for ~15 ms (full width at half maximum of 17 ± 1 msec). We return to the delay of fluctuations in the inputs to OFF cells relative to ON cells in discussing Figure 4 below.

We performed the same experiment by recording simultaneously from an ON midget and an ON parasol ganglion cell. These cells also receive excitatory input from different cone bipolar cell types: ON midget and ON diffuse bipolar cells respectively [25] (Figure 1c, left). Yet excitatory synaptic inputs to nearby ON midget and ON parasol ganglion cells also covaried during constant illumination (Figure 1c, d) with little or no delay between correlated fluctuations in the inputs to the two cell types (peak at 0.0 ± 0.2 ms, mean ± SEM, n=18). The width of the crosscorrelation function (9.2 ± 0.8 ms) was less than that for the ON parasol/OFF parasol pairs but similar to that for ON parasol pairs (8.6 ± 0.7 ms, data from ref. 26).

Correlated noise in the excitatory synaptic inputs to distinct ganglion cell types implies covariation in transmitter release from different bipolar cell types. This covariation could originate from shared cone input to the circuits controlling excitatory inputs to the ganglion cells, or it could arise from noise generated in amacrine cells that contact multiple bipolar cell types. To test whether amacrine inputs are required for correlated noise, we recorded simultaneously from horizontal cells and ganglion cells (Figure 1e). Horizontal cells receive input mainly from photoreceptors and other horizontal cells. Rod input to horizontal cells and ganglion cells was minimal at the light levels used in these experiments (not shown), and therefore should not contribute to shared noise. Nonetheless, excitatory synaptic inputs to horizontal and ON parasol ganglion cells covaried during constant light (Figure 1e, f). Fluctuations in the horizontal cell inputs preceded correlated fluctuations in the ganglion cell inputs (peak at −11 ± 1 ms, mean ± SEM, n=5) with a correlation time (16 ± 1 ms) similar to

that of ON/OFF parasol pairs. Taken together, these results suggest that noise in shared cone inputs is the most likely source of correlated noise in the synaptic inputs to nearby ganglion cells.

The crosscorrelation functions in Figure 1 are all substantially narrower than expected from the ~30–60 ms width of the light-dependent correlations in the cell's inputs (i.e. the width of crosscorrelation functions measured during modulated light input, see right panel of Figure 4b). Thus neither quantal fluctuations in light input nor spontaneous activation of the cone photopigment can account for correlated noise. The properties of correlated noise will be shaped by the circuitry conveying cone signals to ganglion cells, including filtering and rectification. In particular, excitatory synaptic inputs to OFF ganglion cells are substantially more rectified than those to ON ganglion cells [27]. Such rectification can make the timing and strength of correlated noise highly stimulus dependent [26], because different stimuli engage the nonlinearities to different degrees; such stimulus dependence substantially complicates quantitative interpretation. These effects are largely absent in correlated noise measured in ON parasol ganglion cell pairs, and hence we focus on ON ganglion cells below.

Dependence of noise on photoreceptor input

Correlated noise in the responses of cells that share little known circuitry other than the cones suggests that much of the noise is produced in the cones themselves. Below we test this suggestion more directly for ON ganglion cells by suppressing the sensitivity of ON cone bipolar cells to glutamate release from the cones. Under these conditions, noise originating downstream of the cones should persist while noise produced in cone phototransduction and transmitter release should be diminished.

These experiments exploited the reliance of the synapse between cones and ON cone bipolar cells on metabotropic glutamate receptors [28]. We used a mixture of receptor antagonists (LY341495) and agonists (APB) chosen to suppress light responses in ON midget and ON parasol ganglion cells while minimally changing their mean excitatory synaptic input. The mixture of antagonists and agonists was optimized for each cell pair, as in the example titration of Figure 2a (data from LY/APB ratio 2 matched the mean excitatory input without drugs and was used for further analysis). Antagonist/agonist mixtures suppressed the light response of ON parasol ganglion cells by a factor of 5 ± 1 (mean ± SEM, n=7). This approach avoids the potentially confounding effects of applying an agonist or antagonist alone, which could change the ON bipolar resting voltage and hence the activity of ON pathways [29]. Indeed, agonists of ON bipolar glutamate receptors alone produced a prominent decrease in a ganglion cell's holding current and an unexpected response at light offset (Figure 2b and c); both were absent in the antagonist/agonist mixture (see Methods for more details).

The antagonist/agonist approach allowed us to test the importance of cone and post-cone noise by maintaining ON bipolar input to downstream cells while suppressing variations in that input produced by cone noise. Figure 3a–b illustrates this approach in simultaneous recordings of excitatory synaptic inputs to an ON parasol and an ON midget ganglion cell. The antagonist/agonist mixture suppressed light responses of both cells while producing

only a small change in holding current. Correlated noise in the inputs to the cells measured during constant light decreased ~7-fold (Figure 3b). Suppressing bipolar sensitivity to cone transmitter release decreased correlated noise in each of 6 such experiments (Figure 3c), on average by a factor of 7 ± 3 (mean ± SEM, n = 6). The decrease in correlated noise in ON parasol/ON midget pairs did not depend on the exact mixture of agonist and antagonist, persisting when the drugs produced small increases or decreases in the mean excitatory synaptic input.

As a control, we measured the effect of similar antagonist/agonist mixtures on correlated noise in the responses of OFF parasol ganglion cell pairs. Excitatory synaptic inputs to these cells should be largely independent of metabotropic glutamate receptors. Rectification of the excitatory inputs to OFF parasol cells can make correlated noise measured during constant light weaker than that measured in the presence of a modulated light input that increases activity in OFF circuits [26]. Hence, we measured correlated noise in OFF parasol cell pairs during modulated light. We subtracted the average response to multiple repeats of the same light stimulus from the response measured on each individual trial (see Methods for details), and measured the correlations of the resulting residuals [26]. Excitatory synaptic inputs to neighboring OFF parasol cells covaried strongly, but such correlated noise was insensitive (<10% change on average) to metabotropic glutamate receptor antagonist/agonist mixtures (open circles in Figure 3c).

The correlated noise that remained when cone input to ON bipolar cells was suppressed could originate downstream of the cones, could be produced by activity in OFF circuits, and/or could reflect incomplete suppression of cone input to ON bipolar cells. Previous work in salamander retina indicates that circuits relying exclusively on electrical synapses contribute strongly to correlated noise in the ganglion cell responses. To test for a similar effect in primate retina, we suppressed glutamatergic excitatory synaptic inputs to ganglion cells with 10 μM NBQX and 20 μM APV. This reduced correlated noise in ON parasol ganglion cell pairs more than 100-fold (data not shown). Thus while the correlated activity of ON parasol cells is shaped by gap junction coupling [26,30,31], likely via amacrine cells, the coupled cells appear to transmit rather than generate noise.

Suppressing cone input to ON bipolar cells also decreased the total variance of the excitatory synaptic input to ON parasol ganglion cells (Figure 3d) by an average factor of 3.0 ± 0.9 (mean ± SEM of the ratio of control variance to that in LY/APB, n = 7); the mean current in the same cells changed by less than 10% (Figure 3e). Variability in the extent of noise suppression appeared to be at least partially due to a failure to precisely match the mean excitatory input before and during drug exposure: the three experiments with the smallest change in noise were those in which the mean excitatory current increased. Noise that remained when cone input to ON bipolar cells was suppressed was synaptic in origin. Thus suppressing a ganglion cell's synaptic input directly by inhibiting glutamate, GABA and glycine receptors decreased the current variance ~50-fold [26]. Remaining synaptic noise could originate from a source other than cones or could reflect incomplete suppression of cone input to bipolar cells. Taken together, these results indicate that a substantial fraction of the variance in a ganglion cell's excitatory synaptic inputs originates from cone noise - either noise in transduction or statistical variations in cone transmitter release.

Rapid fluctuations in cone voltage are relayed to ganglion cells

The above results indicate that cone noise accounts for the majority of the correlated noise in ganglion cell responses. Previous work, however, has argued that signals initiated in the cones are too slow to account for correlated noise [17,19], and that instead correlated noise likely originates from a distinct circuit. This argument is based on the relatively slow kinetics of cone light responses and the assumption that the kinetics of cone noise is similarly slow. The apparent discrepancy with the current findings can be reconciled if cone noise varies rapidly compared to the cone light response, and if rapid fluctuations in the cone output are able to produce rapid fluctuations in a ganglion cell's synaptic input.

Figure 4a shows fluctuations in the cone voltage measured during constant light and the average cone response to a brief flash. Figure 4b shows autocorrelation functions of the voltage noise and light response. The correlation time of the noise (full width at half maximum of 13 ± 1 ms, mean ± SEM, n = 5) was considerably smaller than that for the light response (49 ± 3 ms). This difference is consistent with past work on the same cells [8] which concluded that much of the noise in the cone voltage originates from sources other than spontaneous or light-activated photopigment.

Signal transfer from cones to ganglion cells was characterized by randomly modulating the cone voltage while recording excitatory synaptic inputs to a ganglion cell (Figure 4c). We correlated the imposed modulation of cone voltage with the resulting modulation of the ganglion cell synaptic input to estimate the transfer function for transmission through the retina. This transfer function (Figure 4c, right) predicts the kinetics of the ganglion cell response to a brief depolarization of the cone. Cone to ON ganglion cell transfer functions (Figure 4d) were briefer than the cone light response (width of 17 ± 2 ms, n = 4). Thus variations in the cone voltage that are more rapid than cone light responses can be transmitted to ON ganglion cells.

The experiments of Figure 4c and d also provided information about the kinetics of signaling in ON and OFF circuits. Specifically, the kinetics of signal transfer from cones to OFF ganglion cells were faster than those from cones to ON ganglion cells: the time-to-peak of transfer function was 8 ± 1 ms for cone-OFF ganglion cell pairs (mean ± SEM, n = 4) and 21 ± 2 ms for cone-ON ganglion cell pairs (n = 4, Figure 4d). The slower kinetics of ON retinal circuits is expected from the comparatively slow metabotropic glutamate receptors expressed by ON bipolar cells [28]. This differs from the conclusion reached from properties of the correlated noise in ON/OFF parasol pairs (Figure 1b), which indicated more rapid transmission to ON ganglion cells. This difference likely arises because nonlinearities in OFF circuits delay small changes in cone output, e.g. those produced by cone noise, while having little effect on large changes in cone output. Indeed, the kinetics of light-dependent modulations of excitatory synaptic inputs to OFF parasol cells were also faster than those to simultaneously recorded ON parasol cells (difference in time to peak of filter 3.9 ± 0.7 ms, mean ± SEM for 9 ON/OFF pairs, $p < 0.001$; Figure 4d). Turtle retina shows a similar asymmetry in transmission through ON and OFF circuits [32].

Cone voltage fluctuations remained correlated longer than noise in the synaptic inputs to nearby ON ganglion cell pairs (correlation function widths of 13 vs 9 ms). At least two

factors could contribute to this difference. First, synaptic noise generated at the cone output synapse could vary more rapidly than fluctuations in cone voltage. Second, slow modulations of cone voltage could be less effective than rapid modulations in producing signals in the ganglion cells - as expected if the kinetics of signal transfer are biphasic. Consistent with this proposal, ganglion cell light responses also have a briefer duration than the cone light response (Figure 4b, right), and the extent of such speeding is consistent with the difference in noise correlation time (not shown). In sum, the experiments of Figure 4 indicate that cone noise varies more rapidly than light responses, and that rapid variations in the cone signals can produce rapid variations in a ganglion cell's synaptic inputs.

Systematic dependence of correlated noise on number of shared cones

The experiments described above suggest a simple picture of how correlated noise is produced: cone noise, relayed through multiple bipolar cell types, causes the responses of ganglion cells with shared cone inputs to covary. To test this hypothesis, we compared the strength of correlated noise in ganglion cell pairs with the degree of shared cone inputs, estimated from their dendritic overlap. Receptive field overlap has little dependence on eccentricity in the peripheral retina where all of our recordings were made [33]; thus systematic changes in circuitry with eccentricity were unlikely to contribute substantially to differences in the degree of shared cone input across cell pairs.

Figure 5a illustrates the model used to predict the strength of correlated noise for an ON parasol/ON midget ganglion cell pair. Model predictions were based on the assumption that all noise originates in the cones, on images of dendritic fields obtained at the end of recordings (Figure 5a, left), and on known properties of the bipolar cells that convey cone input to midget and parasol ganglion cells (see Methods). Signals from each cone in a simulated array (red circles in Figure 5a, right) were spread spatially over an area determined by the size of the axon terminal of the diffuse or midget cone bipolar cells ([25]; shaded red disks in Figure 5a). The weight of the input of an individual simulated cone to a ganglion cell was determined by the length of dendrite within this area, as would be expected if there were a uniform density of synaptic receptors [34,35]. The correlation coefficient of the resulting weights for the two ganglion cells across all cones provided a prediction for the strength of correlated noise.

The observed correlation strength (peak of the crosscorrelation function as in Figure 1d) was close to the model prediction across a wide range of dendritic overlaps (Figure 5c). This agreement held for both ON midget/ON parasol and ON parasol/ON parasol ganglion cell pairs. The dependence of correlation strength on dendritic overlap supports the idea that shared noise accounts for the majority of the noise in the excitatory synaptic inputs to ON midget and ON parasol ganglion cells. If independent noise in the midget and parasol circuits contributed strongly to response variation, the measured correlations would be smaller than the predictions. For example, with equal shared and independent noise, the measured correlations should be half as large as those predicted (line labeled 1:1 in Figure 5c). Shared noise could originate from the jointly sampled cones or from mixing of signals in midget and parasol circuits downstream of the cones; the sensitivity to block of cone input (Figure 3b–c) and the correspondence between the spatial scale of the noise in parasol

circuits and the size of diffuse bipolar cells (Supplementary Figure 1 in ref. 26) argue that most of the shared noise originates in the cones.

The model used to predict correlation strength was kept simple so as not to introduce unnecessary free parameters. The model predictions rely on two assumptions about how bipolar cells integrate and distribute cone signals: (1) that the spread of cone signals is determined by the size of the axon terminal of the relevant bipolar type or types; and (2) that the cone weights to a bipolar cell can be modeled as a uniform disk. The conclusions, however, were robust to reasonable changes in either assumption. Specifically, the measured correlation strength remained above the 1:1 line for all reasonable values of the model parameters, including up to 3x changes in signal spread and Gaussian rather than uniform weighting of cone inputs to bipolar cells (see Figure 7 and Methods for details).

Impact of correlated noise on the representation of light inputs in ganglion cell population

Correlated noise generated by shared cone inputs could alter how faithfully a population of ganglion cells transmits visual information to the brain. For example, correlated noise among neurons can limit the capacity to average their signals and obtain more precise sensory information (e.g. refs. 15, 36). The results described above suggest that such effects should be substantial, although the impact of shared cone signals could also be minimized in some ganglion cell types by circuit nonlinearities. To test these predictions, we determined how the fidelity of stimulus encoding by ganglion cell pairs depended on the extent to which the cells shared cone signals.

We simultaneously recorded the spike responses from populations of ganglion cells (e.g. ON parasol cells in Figure 6a, top) to a spatially uniform, time-varying stimulus that provided the same input to all cells, regardless of their separation. In this case, cell pairs with shared cone inputs should jointly represent the stimulus less accurately than cell pairs without shared cones, because independent noise can be reduced by averaging whereas shared noise cannot. Thus, if all noise originates in the cones, two cells that sample from the same set of cones will have a joint signal-to-noise ratio (SNR) a factor of $\sqrt{2}$ lower than two cells that sample from nonoverlapping cones. Independent noise introduced later in the retinal circuitry will mitigate the effect of shared cone noise.

We reconstructed the time-varying stimulus from the spike responses of each ganglion cell pair using a simple linear decoding scheme (Figure 6a, bottom). We calculated the best linear reconstruction of the stimulus given the spike responses of a pair of cells, and compared this reconstruction to the actual stimulus. The difference between the two, corrected for systematic errors, provided an estimate of the noise in the reconstruction (see Methods for details). The SNR of the reconstruction was defined from the ratio of the stimulus and noise amplitudes. The SNR declined systematically with distance for nearby pairs of cells, consistent with a substantial effect of shared noise on the visual signal (Figure 6b). We repeated this approach for several combinations of parasol and midget ganglion cells (Figure 6c–f).

The dependence of SNR on distance differed systematically for different RGC types (Figure 6b–f). These differences likely reflect two issues: (1) whether ganglion cells integrate cone

signals linearly or nonlinearly; and (2) whether the two ganglion cells contribute symmetrically to the reconstruction. Thresholding or rectifying nonlinearities alter the relative impact of noise introduced at early (pre-nonlinearity) and late (post-nonlinearity) stages of processing, and hence alter the balance of shared and independent noise. Stronger synaptic nonlinearities likely account for the weaker dependence of SNR on receptive field overlap for OFF ganglion cell pairs compared to that for ON parasol pairs (Figure 6b,c). Asymmetries in the signal-to-noise ratio of the two cells, e.g. due to differences in receptive field size in parasol and midget cells (Figure 6e,f), will cause the cell with more cone inputs and hence higher SNR to dominate the reconstruction and make the joint SNR insensitive to shared noise in the two cells. Anticorrelated light responses, as in ON parasol/OFF parasol pairs (Figure 6d), together with nonlinearities, reduce the effects of shared noise since the two cells are rarely coactive. Thus, interestingly, the impact of shared noise in such cases is likely highly stimulus dependent, with the largest effects occurring for weak stimuli. The linearity and symmetry assumptions held most closely for ON parasol pairs, and hence we focused on these cells for further quantitative analysis.

To investigate the relative contributions of shared and independent noise on coding, the dependence of SNR on receptive field overlap was fit with the model of Figure 5, modified to include a separate source of independent noise. Figure 6g compares model predictions (lines) with data from ON parasol cell pairs (Figure 6b). Receptive field overlap was estimated either directly from raw pixel-based receptive field measurements or from Gaussian fits (closed and open points, see Methods). In three preparations, this analysis indicated a greater contribution of shared noise than independent noise, in general agreement with results from Figure 3c and 5. Two issues produce uncertainty in quantitative estimates of the impact of shared noise: (1) inadequacies in the linear reconstruction approach will appear as a source of independent noise; and, (2) the Gaussian receptive field fits overestimate overlap due to interdigitation of the real receptive fields [33], accounting for the dependence on the data in Figure 6g on the method used to measure overlap. Nonetheless, these results indicate that shared noise limits the accuracy with which common light stimuli are represented by neighboring ON parasol cells.

Discussion

The present results provide a common mechanistic understanding of two fundamental properties of retinal signals that govern how visual signals are transmitted to the brain: the fidelity of cone-mediated retinal responses, and correlated activity among retinal ganglion cells. A simple picture emerges: cone noise, traversing the retina through diverse pathways, accounts for most ganglion cell noise and correlations.

The sensitivity of cone-mediated visual signals was recently investigated by Borghuis et al. (2009) in guinea pig retina. Discriminability of small changes in light intensity based on horizontal cell and ganglion cell responses was compared to limits set by statistical fluctuations in photon capture by the cones, assuming linear integration of cone signals at both stages. Horizontal cell sensitivity fell short of limits set by photon capture noise, consistent with physiological noise in cone phototransduction and/or synaptic transmission. Ganglion cell sensitivity was ~3-fold lower (1.7-fold in the most sensitive cells) than

horizontal cell sensitivity, consistent with additional sources of noise in the retina. Assuming equal and additive cone and post-cone noise, a 1.4-fold loss of sensitivity between horizontal cells and ganglion cells would be expected. The larger observed sensitivity loss at the ganglion cells indicates a greater contribution from post-cone noise. The larger role of cone noise observed here could reflect species differences and/or the different experimental and analysis methods.

The present analysis of noise in the retina relies on several technical advances. First, correlated noise was measured directly in several cell types that shared little circuitry other than cones. Second, a novel pharmacological approach was used to suppress the sensitivity of ON bipolar cells to cone noise while maintaining the mean synaptic input from cones. Third, the impact of shared noise on visual signals was tested directly. The current approach is limited primarily by significant nonlinearities that complicate the analysis of correlations in OFF cells [26], the contribution of gap-junction coupling to correlated noise in ON parasol cells [26,30], and the necessity in some experiments of using a slice preparation which removes some amacrine and ganglion cell processes and can alter the kinetics of synaptic transmission.

The present results indicate that shared noise makes a larger contribution to noise in ganglion cell inputs that independent noise; this conclusion held across a broad range of parameters of the noise model used to make the estimates (Figures 5 and 7). Correlated noise required intact signaling between cones and ON cone bipolar cells (Figure 3), indicating that most shared noise originated in the cones themselves. This suggests that the circuitry largely preserves visual information encoded in the cone lattice, and that behavioral sensitivity, e.g. to small changes in color or spatial position, could approach the bounds imposed by cone noise. The comparatively low level of noise introduced as signals are transmitted across the retina reveals high fidelity in synaptic transmission and neural coding. Similar findings regarding the noise in visual signals initiated by rod photoreceptors led to the discovery of a finely coordinated set of biophysical mechanisms mediating the exquisite sensitivity of night vision (reviewed in ref. 37).

Correlated noise in ganglion cells displayed faster kinetics than their light responses. In previous work, this observation led to the hypothesis that correlations arise primarily from divergent noise in a spiking interneuron [17–19]. However, at low light levels a slow component of ganglion cell correlations with a time scale similar to the rod light response suggested an origin in rod noise [16]. The frequency of correlated bursts of action potentials in dark-adapted cat ganglion cells suggested that they originated from thermal activation of photopigment in shared rod inputs [16]. The present results indicate that the situation for rod and cone-mediated signals and correlated noise is similar, and that a common set of circuitry can account for both. Unlike the situation for rods, however, thermal activation of the cone photopigment contributed minimally; instead the dominant noise in the cone output signals originated in either rapid fluctuations in downstream elements of the phototransduction cascade [8] or variability in transmitter release. The rapid time scale of ganglion cell correlations can be explained by the rapid transmission of this cone noise to ganglion cells.

The present work also highlights several similarities and differences in correlated activity in retinas of different species. First, ON and OFF ganglion cells in cat exhibit anticorrelated spike responses such as those seen here [16]; such anticorrelation is less prominent in rabbit ganglion cells, perhaps due to low firing rates under the conditions of the experiments [18]. Second, unlike primate cones, most of the noise in salamander cones has a time scale very similar to the light response [38] and therefore is unlikely to explain rapid correlated activity [19]. Third, circuits that rely entirely on electrical synapses make a greater contribution to correlated activity in salamander retina than was observed here [19].

Multiple mechanisms could convey cone noise to ganglion cells, including common synaptic input and reciprocal coupling through gap junctions between ganglion cells and between amacrine and ganglion cells [30,39–41]. The kinetics and nonlinearities of these mechanisms in turn will shape correlated noise and its stimulus dependence. Further, while cone noise appears to account for the most of the correlated noise in nearby ganglion cells, our results do not preclude other, smaller components with different circuit origins and spatial properties. Indeed the remnant correlated noise observed with cone signals suppressed (Figure 3) suggests that such sources exist.

The retinal output consists of ~15 parallel pathways that encode different aspects of the visual scene (reviewed in refs. 42, 43). Many of these pathways (e.g. ON vs OFF, midget vs parasol) are initiated by the divergence of cone signals to ~10 classes of bipolar cells [25]. Noise in the cones is thus naturally shared across pathways. The resulting covariation in noise between pathways suggests that there is limited benefit to averaging across the outputs of distinct parallel circuits sampling from the same region of space. Therefore, the parallel pathways could remain largely parallel in the brain with relatively little cost in terms of faithful visual representation.

However, downstream circuits in the visual system could minimize the effect of shared cone noise [44], or even exploit it. For example, shared noise could have a relatively small impact on visual signals encoded by the relative timing of spikes in different cells, with potentially important implications for the neural code of the retina [45]. Also, shared noise could be used to keep in temporal register features of the visual scene that occupy the same region of space, because response fluctuations in the collection of neurons encoding that region covary.

Methods

Recordings and solutions—Electrical recordings were made from primate retina as described previously [22,26,43]. All recordings were from peripheral retina (> 20 degrees eccentricity). At these eccentricities, a relatively constant number of cones provide input to a given type of ganglion cell as changes in cone density roughly match changes in ganglion cell dendritic extent. Three different preparations were used. Cones, cone-ganglion cell and horizontal-ganglion cell pairs were recorded in a slice preparation using whole-cell patch clamp techniques. Slicing invariable cut some processes of cells with large dendritic fields, likely slowing the kinetics of synaptic transmission. Intracellular measurements of ganglion cell pairs were made in a flat mount preparation.

Patch pipettes for ganglion cell recordings were filled with an internal solution containing (in mM) 90 $CsCH_3SO_3$, 20 TEA-Cl, 10 HEPES, 10 Cs_2-EGTA, 10 sodium phosphocreatine, 2 QX-314, 4 Mg-ATP and 0.5 Mg-GTP; pH was adjusted to ~7.2 with CsOH and osmolarity was ~280 mOsm. Patch pipettes for cone and horizontal recordings were filled with an internal solution containing (in mM) 125 K-Aspartate, 10 KCl, 10 HEPES, 5 NMG-HEDTA, 1 $MgCl_2$, 0.5 $CaCl_2$, 4 Mg-ATP, 0.5 Tris-GTP; pH was adjusted with NMG-OH. Internal solutions included 0.1 mM of either Alexa 488 or Alexa 555. Holding potentials have been corrected for a −10 mV liquid junction potential. Series resistance in ganglion cell recordings was 10–15 MΩ, and was 50–70% compensated; series resistance in cone recordings was 15–25 MΩ and was not compensated. Excitatory synaptic inputs were isolated by holding a cell near the reversal potential for inhibitory synaptic inputs (~−70 mV). Extracellular measurements of the ganglion cell population were made using an electrode array. During all recordings the retina was perfused at 4–8 ml/min with Ames' solution warmed to 32–35 °C.

To suppress ON bipolar sensitivity to glutamate released from the photoreceptors, we used a mixture of metabotropic glutamate agonists (APB) and antagonists (LY341495). We took this approach because in the presence of APB alone the increase in excitatory input at light onset was suppressed, but the holding current decreased and a prominent response to light offset emerged (Figure 2b, c, blue). We attribute this response to OFF pathway input that is normally suppressed by activity in the ON pathways - e.g. by crossover inhibition. With an appropriate antagonist/agonist mixture, the ganglion cell's holding current matched that normally present, indicating the tonic rate of transmitter release from ON bipolar cells was close to normal (Figure 2b, c). The unexpected response at light offset was absent, likely because tonic output of ON bipolars is maintained. The suppression of current during the step of darkness in control and antagonist/agonist conditions (Figure 2b, red and black) is likely due to inhibitory input to ON bipolar cells generated from OFF circuits.

Agonist and antagonist concentrations were chosen to keep the excitatory synaptic input to a ganglion cell constant. We started with an initial mixture (typically 6 μM LY341495 and 4 μM APB), and adjusted this mixture by ~20% as needed to match the current prior to drug exposure (example of titration in Figure 2a). LY/APB ratios for the data in Figure 3 ranged from 1.5 to 1.85.

The kinetics of signal transfer between cones and ganglion cells (Figure 4) was measured by modulating the cone voltage (gaussian modulations, 0–300 Hz bandwidth, 3–5 mV standard deviation) while recording a ganglion cell's excitatory synaptic input. This modulation in cone voltage is about 10 times larger than the 0.45 ± 0.05 mV random fluctuations produced by transduction noise. This difference is expected, however, since we are modulating the voltage of a single cone, while noise is present in all of the ~100 cones that provide input to a ganglion cell. With linear signal transfer, a 5 mV random modulation of a single cone would produce a ganglion cell response equivalent to 0.5 mV independent random fluctuations in 100 cones. The transfer function between the cone voltage fluctuations and ganglion cell input was determined by crosscorrelation [46]. A similar analysis was used to measure transfer functions between light input and ganglion cell excitatory synaptic currents.

Crosscorrelation functions—Correlated noise was measured by computing crosscorrelation functions for the signals in pairs of cells:

$$C(\tau)=\frac{\langle I_1(t)I_2(t+\tau)\rangle - \langle I_1(t)\rangle\langle I_2(t+\tau)\rangle}{\sqrt{\sigma_1^2\sigma_2^2}},$$

where the averages <···> are over time, I is current and σ^2 is variance. Correlation functions during constant light were computed after excluding data for at least 500 ms following the end of a modulated light stimulus; results were not noticeably changed when this period was extended. Correlated noise during modulated light was calculated by first subtracting the average response to at least 10 trials of the same stimulus from each individual response. Correlation functions of the resulting residuals were calculated as above.

Model predicting correlation strength from dendritic overlap—Images of the dendrites of recorded ganglion cell pairs (e.g. Figure 5a) were used estimate the strength of shared cone input and predict correlation strength. This analysis differed from that in Trong and Rieke (2008), which related correlation strength to dendritic overlap but not shared cone input. Raw fluorescent images were flattened using a maximum-points projection. Dendrites were identified by finding edges in the flattened images using an automated routine with a threshold set by eye for each image. Cones were arranged on a regular hexagonal lattice with an 18 μm spacing estimated from images of the cone mosaic at the locations of recorded ganglion cell pairs.

Midget and parasol ganglion cells receive excitatory input from midget and diffuse cone bipolar cells, respectively. The area of the axon terminal of these bipolar types determines the region of ganglion cell dendrite that receives input from a given cone. Thus cone signals were spread over a disc with a radius of 27 μm for diffuse cone bipolar cells and 9 μm for midget cone bipolar cells [25]. The synaptic weights (w_n^{midget}, $w_n^{parasol}$) for a given cone input n to the parasol and midget ganglion cell were determined by the length of dendrite within these discs. The correlation coefficient of these weights provided an estimate for the strength of correlated noise:

$$C_{pred}=\frac{\sum_n w_n^{midget} w_n^{parasol}}{\sqrt{\sum_n (w_n^{midget})^2 \sum_n (w_n^{parasol})^2}}$$

where the sum is over cones. This prediction assumes correlated noise is determined entirely by the strength of shared cone input.

Conclusions based on model predictions were robust to reasonable changes in model parameters (i.e. the points in a plot analogous to Figure 5c remained above the 1:1 line; see Figure 7). Thus the conclusion that cone noise exceeded post-cone noise in the ganglion cell input held: (1) when bipolar cells were arranged on a grid rather than centered on the cones (Figure 7a); (2) for 50% changes in cone spacing (not shown), and >100% changes in bipolar signal spread (Figure 7b–c); and (3) when the weight of cone inputs to bipolar cells

had a Gaussian rather than uniform distribution (not shown). These changes are much larger than the uncertainty in the anatomical parameters the model is based on.

Joint coding of stimuli by ganglion cell pairs—The fidelity of signals in pairs of ganglion cells was assessed by using their spike responses to linearly reconstruct a spatially uniform white noise stimulus [47,48]. The reconstructed stimulus *R(t)* was formed by convolving the spike train of each cell with a cell-specific linear filter and summing the results - i.e.

$$R(t)=\sum_i F_1(t-t_i)+\sum_j F_2(t-t_j)$$

where F_1 and F_2 are the filters and t_i and t_j the spike times for the two cells. Thus each spike is replaced with the trajectory of the filter, and the sum of the resulting waveforms provides the reconstructed stimulus. The linear filters were chosen together to provide a least-squares estimate of the stimulus. Reconstructions used a segment of the spike data that was not used in computing the filters.

Reconstructions deviated both randomly and systematically from the actual stimulus. Correction for systematic errors was performed by regressing the reconstruction against the true stimulus separately across frequencies. The regression coefficient at a particular frequency measures systematic differences in the scale of the reconstruction and true stimulus. Rescaling the reconstruction by these regression coefficient removes such systematic errors [46]. Noise was defined as the difference between the stimulus and this corrected reconstruction.

The SNR was determined as the ratio of the stimulus to the noise, averaged over the 10 Hz frequency range for which this ratio was maximal. To normalize for the SNR of the individual cells in a pair, the SNR was divided by the value that would be predicted if the cells were statistically independent. The predicted SNR was obtained by regression of the combined SNR of all pairs that should exhibit no shared noise because of their wide separation (>10 receptive field radii, Figure 6b) against the SNR of the individual cells, and application of these regression coefficients to the individual cells in each pair.

Receptive fields (RFs) were measured by reverse correlation with a spatiotemporal white noise stimulus [49]. Receptive field overlap was measured using the inner product of Gaussian fits to the receptive field center divided by the product of their magnitudes. In the second alternative approach, the spatial component of RF was used directly, with analysis restricted to pixels with amplitude exceeding a threshold fraction (1%) of peak amplitude, within a spatially contiguous region including the peak.

Acknowledgments

We thank Greg Horwitz, Gabe Murphy, Liam Paninski and Michael Vidne for detailed comments on the manuscript and helpful discussions, Daniel Carleton, Eric Martinson and Paul Newman for excellent technical assistance, Greg D. Field, Jeffrey L. Gauthier, Jonathon Shlens and Alexander Sher for experimental assistance, Alan M. Litke, Matthew I. Grivich, Dumitru Petrusca, Wladyslaw Dabrowski, A. Grillo, P. Grybos, P. Hottowy and

S. Kachiguine for technical development, and Joanna Crook, Dennis Dacey, Toni Haun, Michael Manookin, Orin Packer, Beth Peterson, Howard Fox and Kent Osborn for providing primate tissue. Support provided by HHMI (FR), NIH (EY-11850 to FR and EY-13150 to EJC), the Academy of Finland (grant 123231 to PAL), the McKnight Foundation (EJC) and a Pioneer Postdoctoral Fellowship Award (MG).

References

1. Mollon JD, Astell S, Cavonius CR. A reduction in stimulus duration can improve wavelength discriminations mediated by short-wave cones. Vision Res. 1992; 32:745–755. [PubMed: 1413557]
2. Westheimer G. Visual hyperacuity. Prog Sens Physiol. 1981; 1:1–30.
3. BARLOW HB. Purkinje shift and retinal noise. Nature. 1957; 179:255–256. [PubMed: 13407693]
4. Donner K. Noise and the absolute thresholds of cone and rod vision. Vision Res. 1992; 32:853–866. [PubMed: 1604854]
5. Barlow HB. Retinal noise and absolute threshold. J Opt Soc Am. 1956; 46:634–639. [PubMed: 13346424]
6. Aho AC, Donner K, Hyden C, Reuter T, Orlov OY. Retinal noise, the performance of retinal ganglion cells, and visual sensitivity in the dark-adapted frog. J Opt Soc Am A. 1987; 4:2321–2329. [PubMed: 3501458]
7. Naarendorp F, et al. Dark light, rod saturation, and the absolute and incremental sensitivity of mouse cone vision. J Neurosci. 2010; 30:12495–12507. [PubMed: 20844144]
8. Schneeweis DM, Schnapf JL. The photovoltage of macaque cone photoreceptors: adaptation, noise, and kinetics. J Neurosci. 1999; 19:1203–1216. [PubMed: 9952398]
9. Fu Y, Kefalov V, Luo DG, Xue T, Yau KW. Quantal noise from human red cone pigment. Nat Neurosci. 2008; 11:565–571. [PubMed: 18425122]
10. Choi SY, et al. Encoding light intensity by the cone photoreceptor synapse. Neuron. 2005; 48:555–562. [PubMed: 16301173]
11. Borghuis BG, Sterling P, Smith RG. Loss of sensitivity in an analog neural circuit. J Neurosci. 2009; 29:3045–3058. [PubMed: 19279241]
12. Mastronarde DN. Correlated firing of retinal ganglion cells. Trends Neurosci. 1989; 12:75–80. [PubMed: 2469215]
13. Meister M. Multineuronal codes in retinal signaling. Proc Natl Acad Sci U S A. 1996; 93:609–614. [PubMed: 8570603]
14. Field GD, Chichilnisky EJ. Information processing in the primate retina: circuitry and coding. Annu Rev Neurosci. 2007; 30:1–30. [PubMed: 17335403]
15. Puchalla JL, Schneidman E, Harris RA, Berry MJ. Redundancy in the population code of the retina. Neuron. 2005; 46:493–504. [PubMed: 15882648]
16. Mastronarde DN. Correlated firing of cat retinal ganglion cells. II. Responses of X-and Y-cells to single quantal events. J Neurophysiol. 1983; 49:325–349. [PubMed: 6300341]
17. Mastronarde DN. Correlated firing of cat retinal ganglion cells. I. Spontaneously active inputs to X- and Y-cells. J Neurophysiol. 1983; 49:303–324. [PubMed: 6300340]
18. DeVries SH. Correlated firing in rabbit retinal ganglion cells. J Neurophysiol. 1999; 81:908–920. [PubMed: 10036288]
19. Brivanlou IH, Warland DK, Meister M. Mechanisms of concerted firing among retinal ganglion cells. Neuron. 1998; 20:527–539. [PubMed: 9539126]
20. Lamb TD, Simon EJ. Analysis of electrical noise in turtle cones. J Physiol. 1977; 272:435–468. [PubMed: 592199]
21. Jackman SL, et al. Role of the synaptic ribbon in transmitting the cone light response. Nat Neurosci. 2009; 12:303–310. [PubMed: 19219039]
22. Dunn FA, Lankheet MJ, Rieke F. Light adaptation in cone vision involves switching between receptor and post-receptor sites. Nature. 2007; 449:603–606. [PubMed: 17851533]
23. Goodchild AK, Ghosh KK, Martin PR. Comparison of photoreceptor spatial density and ganglion cell morphology in the retina of human, macaque monkey, cat, and the marmoset Callithrix jacchus. J Comp Neurol. 1996; 366:55–75. [PubMed: 8866846]

24. Werblin FS, Dowling JE. Organization of the retina of the mudpuppy, Necturus maculosus. II. Intracellular recording. J Neurophysiol. 1969; 32:339–355. [PubMed: 4306897]
25. Boycott BB, Wassle H. Morphological Classification of Bipolar Cells of the Primate Retina. Eur J Neurosci. 1991; 3:1069–1088. [PubMed: 12106238]
26. Trong PK, Rieke F. Origin of correlated activity between parasol retinal ganglion cells. Nat Neurosci. 2008; 11:1343–1351. [PubMed: 18820692]
27. Zaghloul KA, Boahen K, Demb JB. Different circuits for ON and OFF retinal ganglion cells cause different contrast sensitivities. J Neurosci. 2003; 23:2645–2654. [PubMed: 12684450]
28. Slaughter MM, Miller RF. 2-amino-4-phosphonobutyric acid: a new pharmacological tool for retina research. Science. 1981; 211:182–185. [PubMed: 6255566]
29. Renteria RC, et al. Intrinsic ON responses of the retinal OFF pathway are suppressed by the ON pathway. J Neurosci. 2006; 26:11857–11869. [PubMed: 17108159]
30. Dacey DM, Brace S. A coupled network for parasol but not midget ganglion cells in the primate retina. Vis Neurosci. 1992; 9:279–290. [PubMed: 1390387]
31. Shlens J, Rieke F, Chichilnisky E. Synchronized firing in the retina. Curr Opin Neurobiol. 2008; 18:396–402. [PubMed: 18832034]
32. Baylor DA, Fettiplace R. Kinetics of synaptic transfer from receptors to ganglion cells in turtle retina. J Physiol. 1977; 271:425–448. [PubMed: 200737]
33. Gauthier JL, et al. Uniform signal redundancy of parasol and midget ganglion cells in primate retina. J Neurosci. 2009; 29:4675–4680. [PubMed: 19357292]
34. Cohen E, Sterling P. Parallel Circuits from Cones to the On-Beta Ganglion Cell. Eur J Neurosci. 1992; 4:506–520. [PubMed: 12106337]
35. Xu Y, Vasudeva V, Vardi N, Sterling P, Freed MA. Different types of ganglion cell share a synaptic pattern. J Comp Neurol. 2008; 507:1871–1878. [PubMed: 18271025]
36. Shadlen MN, Britten KH, Newsome WT, Movshon JA. A computational analysis of the relationship between neuronal and behavioral responses to visual motion. J Neurosci. 1996; 16:1486–1510. [PubMed: 8778300]
37. Field GD, Sampath AP, Rieke F. Retinal processing near absolute threshold: from behavior to mechanism. Annu Rev Physiol. 2005; 67:491–514. [PubMed: 15709967]
38. Hamer RD, Nicholas SC, Tranchina D, Liebman PA, Lamb TD. Multiple steps of phosphorylation of activated rhodopsin can account for the reproducibility of vertebrate rod single-photon responses. J Gen Physiol. 2003; 122:419–444. [PubMed: 12975449]
39. Vaney DI. Many diverse types of retinal neurons show tracer coupling when injected with biocytin or Neurobiotin. Neurosci Lett. 1991; 125:187–190. [PubMed: 1715532]
40. Hu EH, Bloomfield SA. Gap junctional coupling underlies the short-latency spike synchrony of retinal alpha ganglion cells. J Neurosci. 2003; 23:6768–6777. [PubMed: 12890770]
41. Hidaka S, Akahori Y, Kurosawa Y. Dendrodendritic electrical synapses between mammalian retinal ganglion cells. J Neurosci. 2004; 24:10553–10567. [PubMed: 15548670]
42. Dacey DM, Packer OS. Colour coding in the primate retina: diverse cell types and cone-specific circuitry. Curr Opin Neurobiol. 2003; 13:421–427. [PubMed: 12965288]
43. Field GD, et al. Spatial properties and functional organization of small bistratified ganglion cells in primate retina. J Neurosci. 2007; 27:13261–13272. [PubMed: 18045920]
44. Pillow JW, et al. Spatio-temporal correlations and visual signalling in a complete neuronal population. Nature. 2008
45. Gollisch T, Meister M. Rapid neural coding in the retina with relative spike latencies. Science. 2008; 319:1108–1111. [PubMed: 18292344]
46. Rieke, F. Spikes: exploring the neural code. MIT Press; Cambridge, Mass: 1997.
47. Bialek W, Rieke F, de Ruyter van Steveninck RR, Warland D. Reading a neural code. Science. 1991; 252:1854–1857. [PubMed: 2063199]
48. Warland DK, Reinagel P, Meister M. Decoding visual information from a population of retinal ganglion cells. J Neurophysiol. 1997; 78:2336–2350. [PubMed: 9356386]
49. Chichilnisky EJ. A simple white noise analysis of neuronal light responses. Network. 2001; 12:199–213. [PubMed: 11405422]

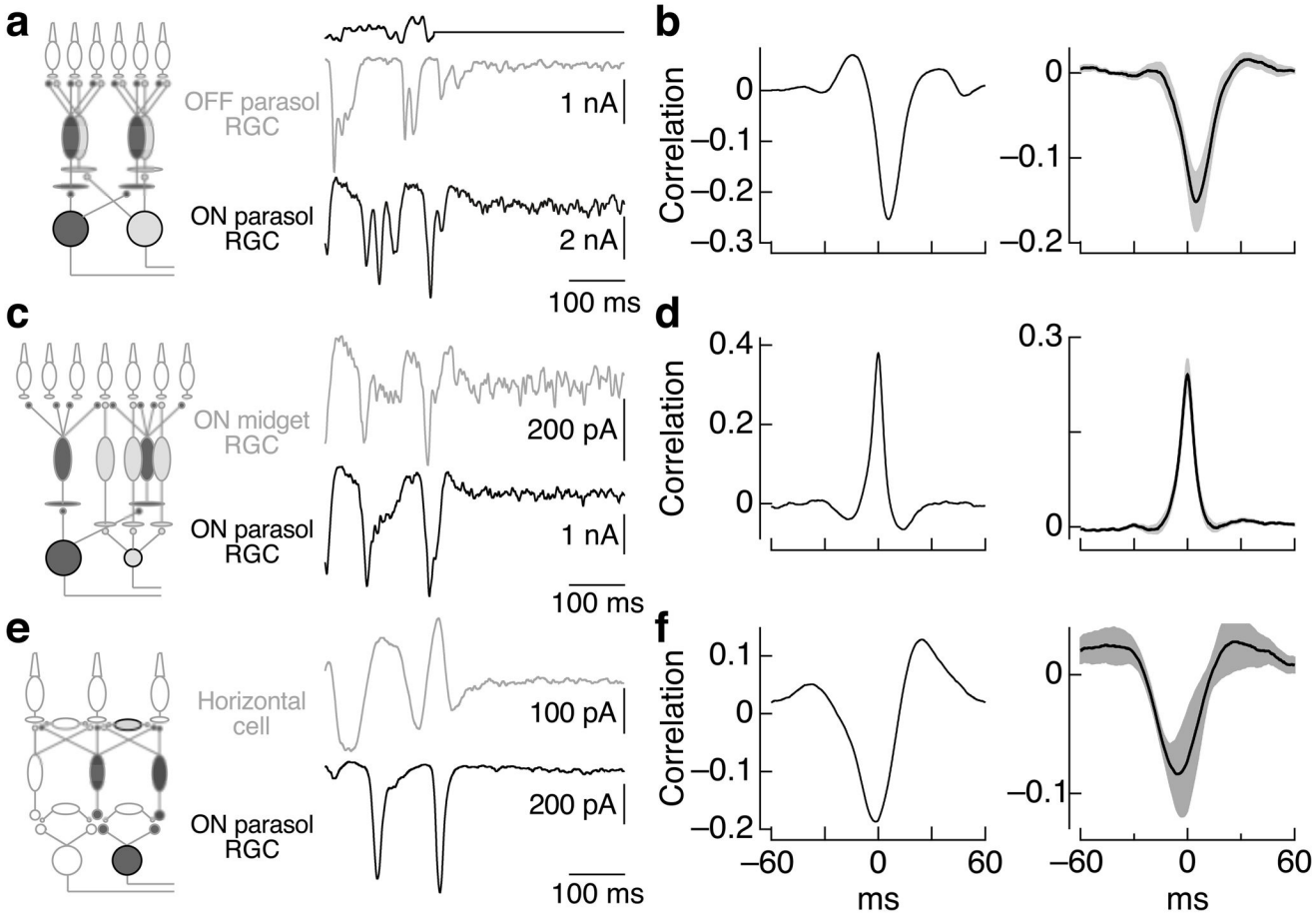

Figure 1.

Covariation of excitatory inputs to cells that share little known circuitry. **a**. Simultaneous recordings of excitatory synaptic inputs to an ON and an OFF parasol ganglion cell during modulated and constant light (top trace; 50% contrast, mean 4000 R*/cone/sec). Holding potentials were ~−70 mV. **b**. Crosscorrelation functions for the excitatory synaptic inputs measured during constant light (excluding 500 ms following the end of modulate light period; see Methods) from the same cell pair as **a** (left) and averaged across 9 cell pairs (right; mean ± SEM). **c, d**. Correlations in excitatory synaptic inputs to ON midget and ON parasol ganglion cells as in **a** and **b** (n = 18). **e**, **f**. Correlations in excitatory synaptic inputs to horizontal cells and ON parasol ganglion cells as in **a** and **b** (n = 5). Recordings for **a–d** were in flat mount preparations, and those in **e** and **f** were in slice preparations.

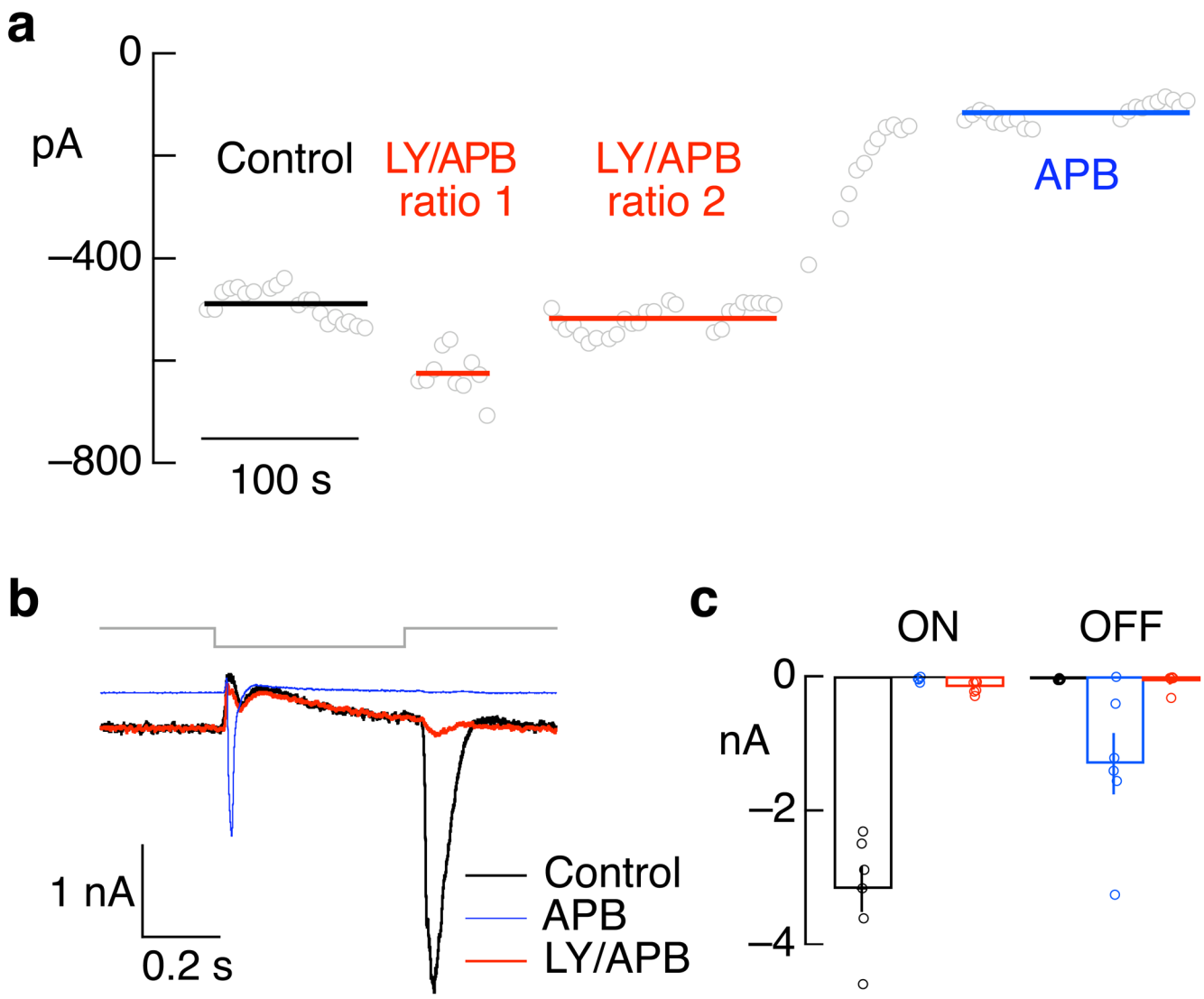

Figure 2.

Effect of APB and mixture of LY341495 and APB on light responses of ON parasol ganglion cells. **a**. Example of titration of mixture of LY341495 and APB to match the holding current without drugs. Open circles plot current in constant light (4000 R*/cone/sec) while holding the cell near the reversal potential for inhibitory synaptic input. The cell was superfused with solutions containing 7.5 μM LY341495 and 2.5 μM APB (ratio 1), 7.5 μM LY341495 and 5 μM APB (ratio 2) and 10 μM APB. **b**. Excitatory synaptic inputs to an ON parasol cell elicited by a decrement in light intensity from 4000 to 0 R*/cone/sec for 500 ms. Increases in light intensity generated large excitatory inputs in control conditions. APB decreased the holding current by suppressing tonic excitatory input, eliminated the response to increases in light intensity, and unmasked a large response to decreases in light intensity. A mixture of LY and APB almost entirely suppressed increases in excitatory input for both decreases and increases in light intensity while also matching the holding current in control conditions. Much of the current change remaining in LY/APB likely reflects OFF pathway derived presynaptic inhibition, which decreases bipolar cell glutamate release. **c**. Collected

data from 6 cells as in **a**, plotting the maximum light-evoked inward current at light onset (ON) and offset (OFF).

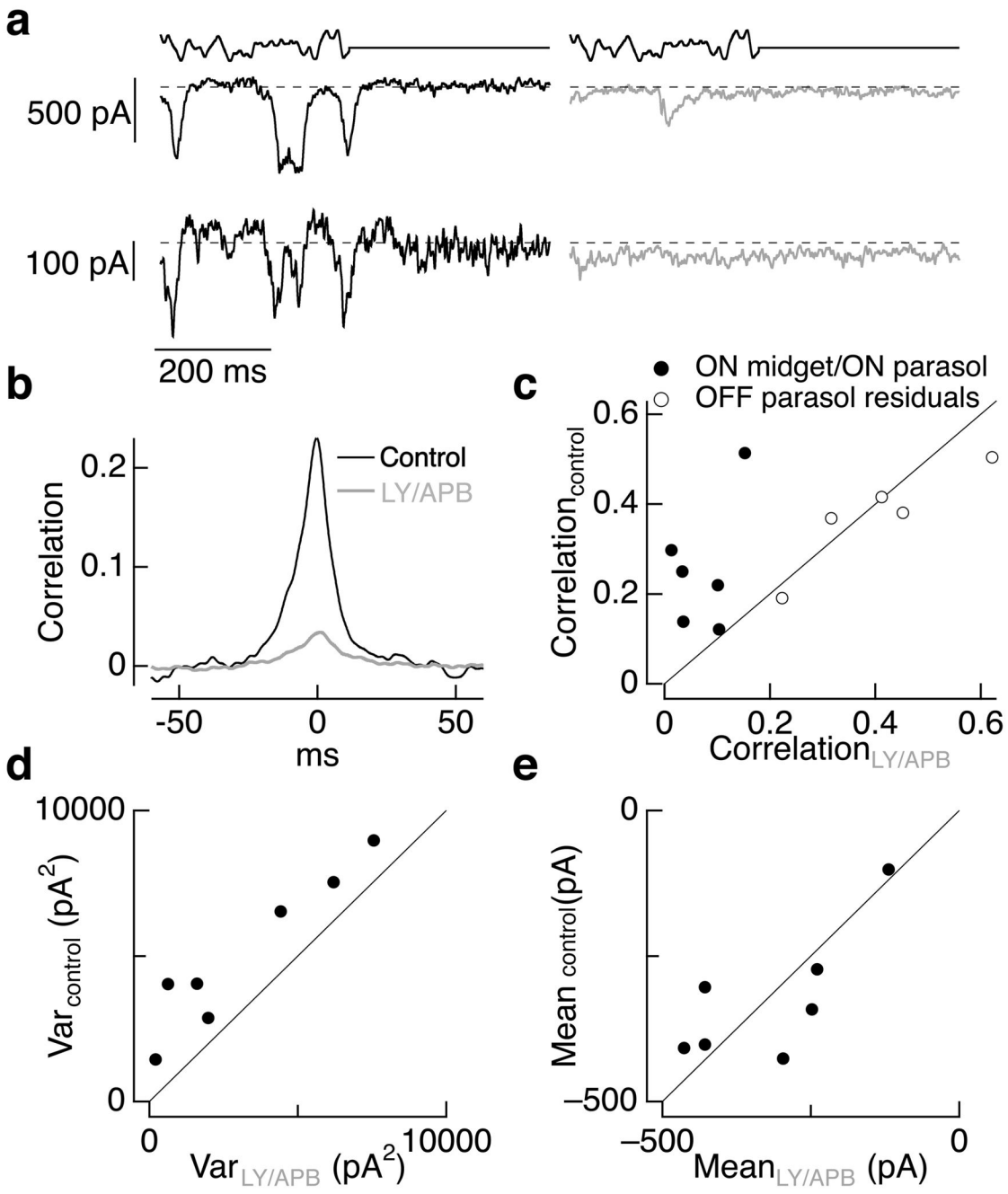

Figure 3.

Correlated and total noise in ganglion cell excitatory synaptic inputs are dominated by cone noise. **a**. Simultaneous recordings of excitatory synaptic input to an ON parasol (top) and an ON midget (bottom) ganglion cell before (left) and during (right) superfusion with a mix of 7.5 μM LY341495 and 4 μM APB. Dashed line shows the mean current level in constant light (4000 R*/cone/sec) prior to exposure to the drugs. **b**. Crosscorrelation functions measured during constant light before (black) and during (red) LY/APB for the same cell pair as **a. c**. Peak crosscorrelation before LY/APB exposure plotted against that during LY/APB for 6 ON parasol/ON midget cell pairs. Also shown are peak crosscorrelations for

5 OFF parasol pairs as a control; correlations were measured from the residuals during modulated light to minimize the effects of nonlinearities in the OFF circuitry (see Methods and ref. 26). **d**. Current variance from 0–100 Hz measured in ON parasol ganglion cells during control conditions plotted against that in LY/APB (including some recordings from single cells not in **c**). **e**. Mean currents during control conditions and LY/APB for the cells in **d**. The mean current in control conditions was 1.05 ± 0.10 times that in LY/APB.

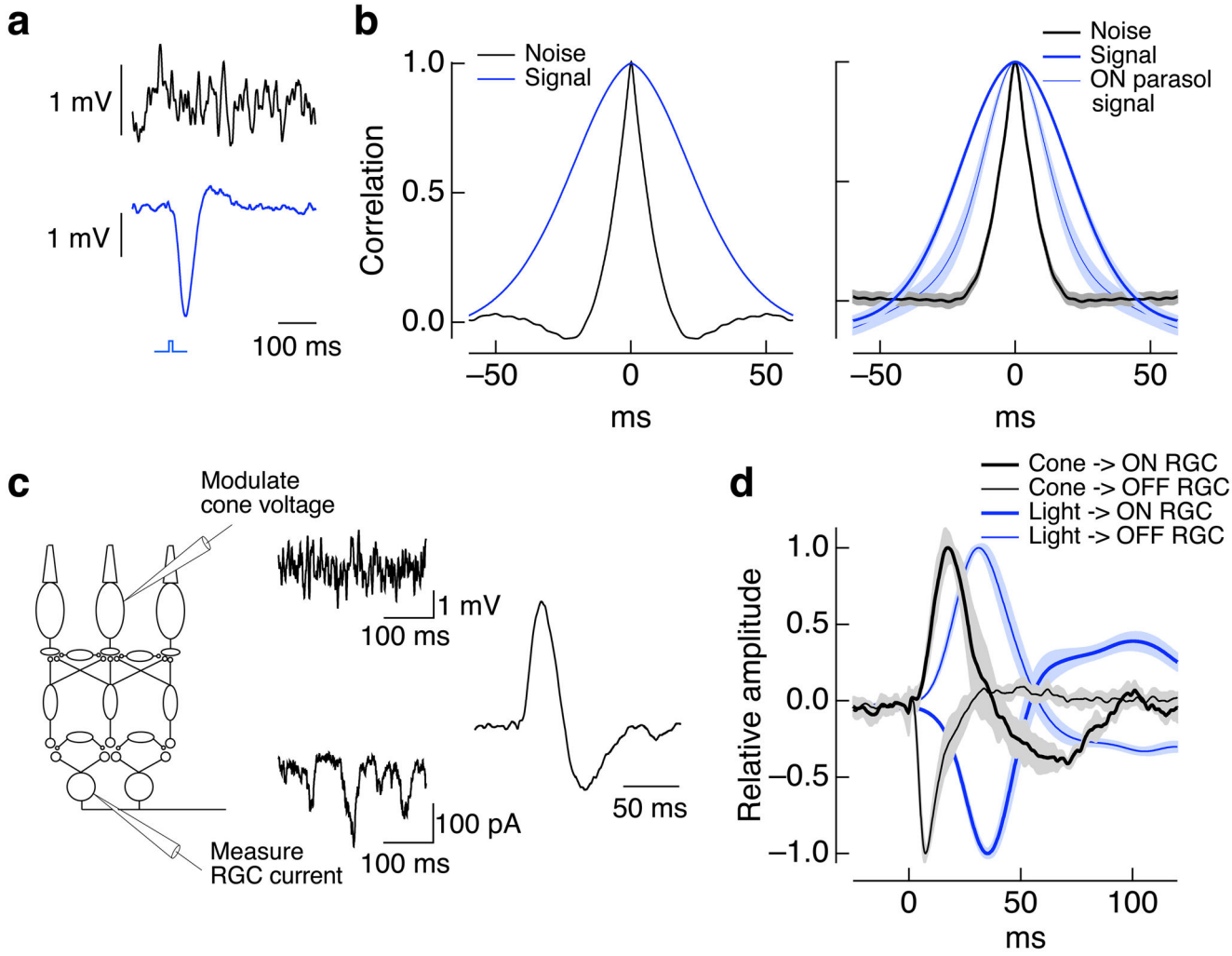

Figure 4.

Rapid fluctuations in cone voltage are conveyed to ganglion cells. **a**. Cone voltage fluctuates more rapidly than the light response. Brief section of voltage fluctuations during constant light (top) and average response to a 10 ms flash (bottom) of a current-clamped cone. Recordings were made at a mean light level of 4000 R*/cone/sec. **b**. (left) Autocorrelation function of noise and light response for the same cone as in **a**. (right) Average autocorrelation functions for 5 cones. For comparison, the autocorrelation function of the light-evoked response of ON parasol cells is also plotted; its narrower width when compared to the cone light response indicates substantial high-pass filtering in the retinal circuitry. **c**. Measurement of kinetics of signal transfer from cones to ganglion cells. The voltage of a single cone was modulated randomly while measuring the resulting variations in excitatory synaptic input to an ON parasol ganglion cell. The cone voltage modulations shown have been filtered for illustration to make the slower modulations more apparent. The kinetics of signal transfer were estimated by calculating the filter that provides the best linear estimate of the ganglion cell currents given the cone voltage (right). **d**. Average filters for paired recordings between cones and OFF parasol cells (n = 4) and cones and ON parasol cells (n = 4). The filters predicting the ganglion cell currents from the light inputs are shown for

comparison (based on 9 recordings from ON/OFF parasol pairs). The opposite polarity of the cone→RGC and light→RGC filters are expected because increases in light input hyperpolarize rather than depolarize the cones.

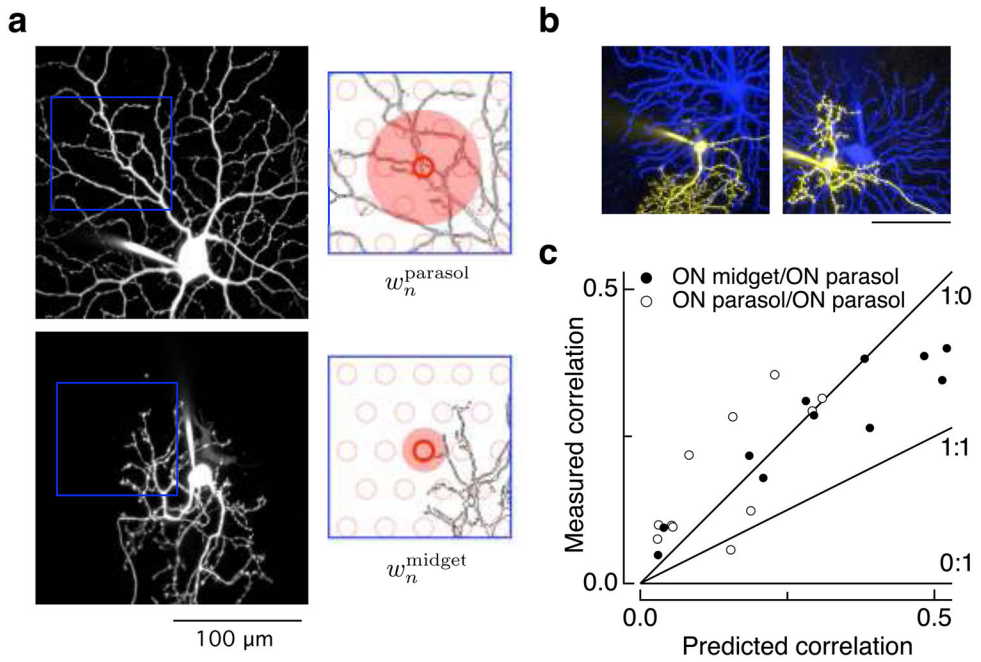

Figure 5.

Dendritic overlap predicts correlation strength. **a**. Maximum-points projections of confocal images of parasol (top left) and midget (bottom left) ganglion cells. The images cover the same region of space but have been separated for clarity. The right panels show discretized regions of the dendrites with a model of the cone array (open red circles) overlaid. The weight of a given cone input to each ganglion cell was estimated from the length of dendrite within an area around the cone determined by the size of the axon terminals of the diffuse and midget cone bipolar cells (shaded red regions) that convey cone signals to parasol and midget ganglion cells. **b**. Midget-parasol ganglion cell pairs with low (left) and high (right) dendritic overlap. **c**. Relation between measured strength of correlated variability in excitatory inputs to midget and parasol ganglion cell pairs (as in Figure 1) and predicted correlation based on model outlined in **a**. Open circles show same analysis for ON parasol pairs. Lines show the expected dependence of correlation strength on overlap for models with different ratios of shared and independent noise as indicated in the labels (shared:independent). Recordings were made at a mean light level of 4000 R*/cone/sec.

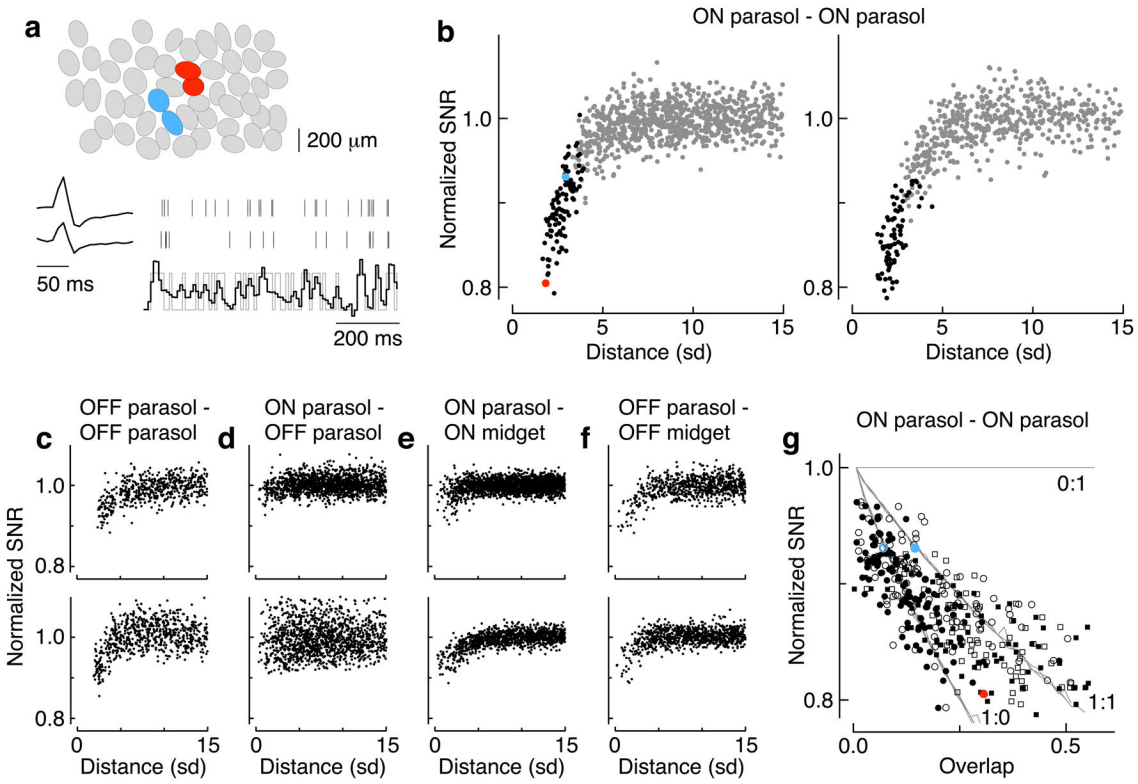

Figure 6.

Shared noise limits fidelity of neural coding in populations of ganglion cells. **a**. Ovals in the top panel represent Gaussian approximation of the receptive fields of simultaneously-recorded ON parasol cells. Pairs of parasol cells were used to reconstruct a time-varying, spatially uniform light input (gray trace, bottom). The spike response of each cell was convolved with an appropriate linear filter and the output summed to generate the reconstruction (black trace). Cell pairs in red and blue are highlighted in **b** and **g. b**. Dependence of signal-to-noise ratio (SNR) of the reconstruction on distance between the two cells, measured in units of the receptive field radius (SD, see top panel in **a**). The SNR is normalized so that pairs of cells that sample independent noise reach a value of one, as determined in distant cell pairs. Neighboring cell pairs are in black. Red and blue points represent cell pairs in **a**. The two panels are two different preparations. **c–f**. Analysis as in **b** for combinations of parasol and midget cells in two preparations. **g**. Dependence of SNR on receptive field overlap for ON parasol pairs. Lines show the expected dependence of SNR on overlap for models with different ratios of shared to independent noise. Closed symbols show overlap measured by correlating each pixel of raw receptive field measurements; open symbols show overlap estimated from Gaussian receptive field fits. Red and blue points represent cell pairs in **a**. Circles and squares represent different preparations from **b**. The mean light level was 1200 R*/cone/sec.

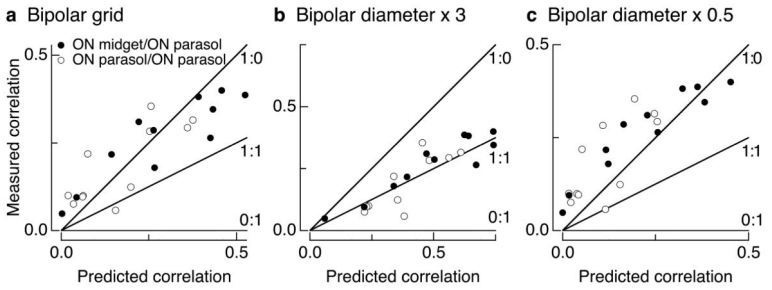

Figure 7.

Dependence of predicted correlation strength on model parameters. Each panel compares predicted and measured correlation strength as in Figure 5c. **a**. Model in which bipolar cells are arranged on a grid and cones provide input to closest bipolar cells. All other parameters as in Figure 5c. **b**. Model in which bipolar cells spread signals over a 81 (27) μm radius disc for the diffuse (midget) cone bipolar cells. **c**. Model in which bipolar signal spread was 13.5 (4.5) μm for the diffuse (midget) cone bipolar cells.